# Interlayer-Coupling-Driven High-Temperature Superconductivity in $La_3Ni_2O_7$ under Pressure

Chen Lu,[1,*] Zhiming Pan,[2,1,*] Fan Yang,[3,†] and Congjun Wu[1,2,4,5,‡]
[1]New Cornerstone Science Laboratory, Department of Physics, School of Science, Westlake University, Hangzhou 310024, Zhejiang, China
[2]Institute for Theoretical Sciences, Westlake University, Hangzhou 310024, Zhejiang, China
[3]School of Physics, Beijing Institute of Technology, Beijing 100081, China
[4]Key Laboratory for Quantum Materials of Zhejiang Province, School of Science, Westlake University, Hangzhou 310024, Zhejiang, China
[5]Institute of Natural Sciences, Westlake Institute for Advanced Study, Hangzhou 310024, Zhejiang, China

(Received 4 August 2023; revised 13 March 2024; accepted 15 March 2024; published 5 April 2024)

The newly discovered high-temperature superconductivity in $La_3Ni_2O_7$ under pressure has attracted a great deal of attention. The essential ingredient characterizing the electronic properties is the bilayer $NiO_2$ planes coupled by the interlayer bonding of $3d_{z^2}$ orbitals through the intermediate oxygen atoms. In the strong coupling limit, the low-energy physics is described by an intralayer antiferromagnetic spin-exchange interaction $J_\parallel$ between $3d_{x^2-y^2}$ orbitals and an interlayer one $J_\perp$ between $3d_{z^2}$ orbitals. Taking into account Hund's rule on each site and integrating out the $3d_{z^2}$ spin degree of freedom, the system reduces to a single-orbital bilayer $t$-$J$ model based on the $3d_{x^2-y^2}$ orbital. By employing the slave-boson approach, the self-consistent equations for the bonding and pairing order parameters are solved. Near the physically relevant $\frac{1}{4}$-filling regime (doping $\delta = 0.3 \sim 0.5$), the interlayer coupling $J_\perp$ tunes the conventional single-layer $d$-wave superconducting state to the $s$-wave one. A strong $J_\perp$ could enhance the interlayer superconducting order, leading to a dramatically increased $T_c$. Interestingly, there could exist a finite regime in which an $s + id$ state emerges.

DOI: 10.1103/PhysRevLett.132.146002

Since the discovery of the high-temperature superconductivity (SC) in cuprates [1], understanding the pairing mechanism of unconventional SC [2–6] and searching for new superconductors with high critical temperature $T_c$ remain long-term challenges. It has been widely believed that strong electron correlations drive the $d$-wave pairing symmetry in high-$T_c$ superconductors [2–4]. Under such an understanding, many attempts have been made to search for high-$T_c$ superconductors in materials with strong electron correlations, especially, the $3d$-transition metal oxides [7–13]. However, no new family of superconductors has been synthesized with $T_c$ above the nitrogen boiling point until the recent discovery of $La_3Ni_2O_7$ (LNO) [14]. It exhibits the superconducting $T_c \approx 80$ K under pressures over 14 GPa, which has attracted considerable attention both experimental [15–17] and theoretical [18–33].

Similarly to cuprates, LNO hosts a layered structure [14–16] with each unit cell containing two conducting $NiO_2$ layers, which is isostructural with the $CuO_2$ layer in cuprates. Calculations based on the density-functional theory (DFT) [14,34] suggest that the low-energy degrees of freedom near the Fermi level are of the Ni-$3d$ orbitals, including two $E_g$ orbitals, i.e., $3d_{z^2}$ and $3d_{x^2-y^2}$, and the site energy of the former is lower than that of the latter. The four $E_g$ orbitals in two $Ni^{2.5+}$ cations within a unit cell share three electrons in total. The $3d_{z^2}$ orbitals in the two layers within a unit cell couple via the hybridization with the O-$2p$ orbitals in the intercalated LaO layer. Under pressure, such a Ni—O—Ni bonding angle along the $c$ axis changes from 168° to 180° [14], which greatly enhances the effective interlayer coupling, as suggested by the combination of the synchrotron x-ray diffraction and DFT calculations [14]. The high-$T_c$ SC only emerges under pressure, implying that the interlayer coupling is crucial for the high-$T_c$ SC in LNO.

The $3d$-orbital character of the low-energy degrees of freedom in LNO suggests strong electron correlations. Such a viewpoint is supported by a recent experiment [15] which reveals that LNO is in the proximity of Mott phase and exhibits non-Fermi-liquid behavior. Therefore, the strong-coupling picture should be legitimate for exploring the pairing mechanism therein. It has been proposed in Refs. [24,33] that the interlayer coupling between the two Ni-$3d_{z^2}$ orbitals along the rung within a unit cell would induce the antiferromagnetic (AFM) superexchange interaction. The same viewpoint is adopted here. However, an important ingredient has been missed in these studies, i.e., Hund's rule coupling between the $3d_{z^2}$ and the $3d_{x^2-y^2}$

 

orbitals within the same $Ni^{2.5+}$ cation, whose effect will be considered in the present study.

In this Letter, strongly correlated models are constructed to investigate the pairing mechanism to LNO under pressure. The two half-filled $3d_{z^2}$ orbitals in a unit cell are viewed as two insulating spins which couple via the interlayer AFM superexchange interaction $J_\perp$ [24,33], while the two quarter-filled $3d_{x^2-y^2}$ orbitals take the role of charge carriers. Under Hund's rule coupling, the AFM interlayer superexchange interaction between two $3d_{z^2}$ orbitals is transmitted to that between two $3d_{x^2-y^2}$ orbitals on two Ni sites along a rung. In combination with the intralayer superexchange interaction, we arrive at a bilayer $t$-$J$ model [35–38] with the single $3d_{x^2-y^2}$ orbital, which is responsible for the SC in LNO. Within the slave-boson mean-field (SBMF) theory [3,4], this model is solved to obtain the ground-state phase diagram and superconducting order parameters. Our result suggests that in the doping regime relevant to experiments, the original intralayer $d$-wave pairing at $J_\perp = 0$ is changed into the interlayer $s$-wave pairing by a realistic value of $J_\perp$. Adopting realistic parameters obtained from DFT calculations [18], our results reveal that the pairing strength is dramatically enhanced by the interlayer AFM coupling relative to that for the single-layered case, which may well explain the origin of the high $T_c$ SC observed in LNO under pressure [14]. Our results further suggest that electron doping into the material will significantly enhance superconductivity.

*Model.*—On average the electron numbers in each $3d_{z^2}$ orbital and $3d_{x^2-y^2}$ orbital are 1 and 0.5, corresponding to half filling and 1/4 filling, respectively. Owing to Hund's rule, electrons in $3d_{z^2}$ and $3d_{x^2-y^2}$ orbitals on the same Ni site tend to form a spin-triplet state. The $3d_{x^2-y^2}$ orbital lies within the $NiO_2$ layer, and its interlayer hopping $t_\perp$ nearly vanishes. The bilayer coupling is through the electron hopping of the $3d_{z^2}$ orbital, intermediated by the $2p$ orbital of the interlayer O atom. The hopping strength could be significantly enhanced under pressure [14]. In the strong coupling limit, the superexchange mechanism induces an effective interlayer AFM spin exchange $J_\perp$ between two $3d_{z^2}$ electrons [24,33]. The electronic properties are described by a two $E_g$-orbital bilayer $t$-$J$-$J_H$ model, as depicted in Fig. 1(a).

The model Hamiltonian is $H = H_\parallel + H_\perp$, with

$$H_\parallel = -t\sum_{\langle \boldsymbol{ij}\rangle,\alpha,\sigma}(c^\dagger_{i\alpha\sigma}c_{j\alpha\sigma} + \text{H.c.}) + J_\parallel\sum_{\langle \boldsymbol{ij}\rangle,\alpha}\boldsymbol{S}_{i\alpha}\cdot\boldsymbol{S}_{j\alpha}$$
$$H_\perp = -J_H\sum_{\boldsymbol{i},\alpha}\boldsymbol{S}_{i\alpha}\cdot\boldsymbol{S}_{z^2 i\alpha} + J_\perp\sum_{\boldsymbol{i}}\boldsymbol{S}_{z^2 i1}\cdot\boldsymbol{S}_{z^2 i2}. \quad (1)$$

Here $c^\dagger_{i\alpha\sigma}$ creates a $3d_{x^2-y^2}$ electron with spin $\sigma$ on lattice site $\boldsymbol{i}$ in the layer $\alpha = 1, 2$. $\boldsymbol{S}_{i\alpha} = \frac{1}{2}c^\dagger_{i\alpha\sigma}[\boldsymbol{\sigma}]_{\sigma\sigma'}c_{i\alpha\sigma'}$ is the spin operator for the $3d_{x^2-y^2}$ orbital, with Pauli matrix $\boldsymbol{\sigma} = (\sigma_x, \sigma_y, \sigma_z)$. The summation $\langle \boldsymbol{ij}\rangle$ takes over all the nearest-neighboring (NN) bonds. Hence, $H_\parallel$ describes two separate layers of the conventional $t$-$J$ model of $3d_{x^2-y^2}$ electrons with a hopping $t$ term and an AFM spin-exchange $J_\parallel$ term. $\boldsymbol{S}_{z^2 i\alpha}$ is the spin operator of the localized single-occupied $3d_{z^2}$ orbital. Therefore, $H_\perp$ describes the coupling of two $t$-$J$ layers through Hund's rule coupling $J_H$ between two $E_g$ orbitals and the interlayer AFM superexchange $J_\perp$ between the $3d_{z^2}$-orbital spins within two layers.

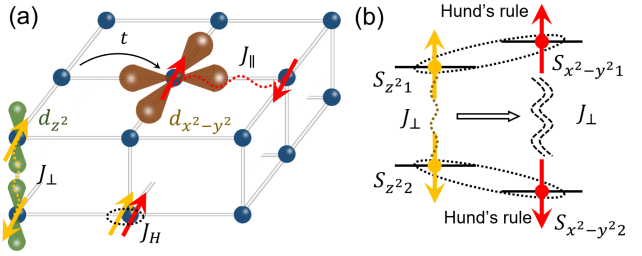


FIG. 1. (a) Schematic diagram for the two-orbital bilayer $t$-$J$-$J_H$ model. The charge carriers reside on the $3d_{x^2-y^2}$ orbitals. The $3d_{z^2}$ orbital is a singly occupied localized spin with interlayer spin exchange $J_\perp$. Two on site $E_g$ orbitals tend to form a spin triplet due to Hund's rule coupling $J_H$. (b) Schematic diagram showing the effective AFM interlayer superexchange interaction $J_\perp$ between the $3d_{x^2-y^2}$ orbitals transmitted from that between the $3d_{z^2}$ orbitals via the on site Hund's rule coupling $J_H$.

This two-orbital problem can be further simplified into a single $3d_{x^2-y^2}$-orbital one since realistically $J_H \gg J_{\parallel,\perp}$. In this limit, the electron spin in $3d_{x^2-y^2}$ will always be aligned in the directions of $\boldsymbol{S}_{z^2 i\alpha}$ in the same cation, and consequently the AFM interlayer superexchange interaction between the $3d_{z^2}$ spins will be transmitted to the $3d_{x^2-y^2}$ electrons, as depicted in Fig. 1(b). This insight can be verified under the framework of the spin-coherent-state path integral [39] given in the Supplemental Material, Sec. A [40]: Integrating out the spin degree of freedom of the $3d_{z^2}$ orbital $\boldsymbol{S}_{z^2 i\alpha}$, an effective interlayer spin-exchange between $3d_{x^2-y^2}$ electrons emerges in the semiclassical approximation. Alternatively, this viewpoint can also be checked in the operator formulation provided in the Supplemental Material, Sec. B [40]: In the large $J_H$ limit, the $3d_{x^2-y^2}$ and $3d_{z^2}$ orbitals on the same $Ni^{2.5+}$ cation form a spin triplet. When acting on this restricted spin-triplet Hilbert space, the spin exchange interaction $\boldsymbol{S}_{z^2 1}\cdot\boldsymbol{S}_{z^2 2}$ is equivalent to $\boldsymbol{S}_1\cdot\boldsymbol{S}_2$. The remaining theory is a bilayer single $3d_{x^2-y^2}$-orbital $t$-$J$ model with the nearest-neighbor spin exchange,

$$H = -t\sum_{\langle \boldsymbol{ij}\rangle,\alpha,\sigma}(c^\dagger_{i\alpha\sigma}c_{j\alpha\sigma} + \text{H.c.}) + J_\parallel\sum_{\langle \boldsymbol{ij}\rangle,\alpha}\boldsymbol{S}_{i\alpha}\cdot\boldsymbol{S}_{j\alpha}$$
$$- t_\perp\sum_{i\sigma}(c^\dagger_{i1\sigma}c_{i2\sigma} + \text{H.c.}) + J_\perp\sum_{\boldsymbol{i}}\boldsymbol{S}_{i1}\cdot\boldsymbol{S}_{i2}. \quad (2)$$

Equation (2) constitutes a minimal model for the mechanism to SC in LNO.

In the following study, $t$ is set as the energy unit. The superexchange interaction $J_\parallel = 4t^2/U$, where $U$ is the Hubbard interaction in the $3d_{x^2-y^2}$ orbital. In this Letter, $U = 10t$ is taken, and hence $J_\parallel = 0.4t$. Other choices of $J_\parallel$ will not change the conclusions. As for $J_\perp$, we will first set $J_\perp/J_\parallel$ as a tuning parameter to fully investigate its effect, and then estimate its realistic value from DFT calculations. In LNO, it is expected that $J_\perp/J_\parallel > 1$. Note that a small interlayer hopping $t_\perp = 0.05t$ is added to pin down the relative pairing phase between the two layers.

*The ground-state phase diagram.*—We employ the SBMF theory [3,4] to solve with the above bilayer $t$-$J$ model (2) (see the Supplemental Material, Sec. C [40] for details). The electron operator is decomposed into $c^\dagger_{i\alpha\sigma} = f^\dagger_{i\alpha\sigma} b_{i\alpha}$, where $f^\dagger_{i\alpha\sigma}/b_{i\alpha}$ is the creation (annihilation) operator of spinon (holon). At the mean-field (MF) level, the spinon and holon degrees of freedom are decoupled. In the ground state, the holons are Bose-Einstein condensed (BEC), and thus their operators are simplified as $b_{i\alpha} = \sqrt{\delta}$, where the hole-doping level $\delta$ is defined as twice of the deviation from half filling and is related to the filling fraction $x$ via $\delta = 1\text{–}2x$. In the ideal case, the filling fraction should be $x = 0.25$. However, in realistic materials, considering the hybridization between the $3d_{x^2-y^2}$ and the $3d_{z^2}$ orbitals [33], as well as the fact that some holes can reside on the oxygen anions [27], the filling fraction can be above 0.25. In this calculation, we set $x \in (0.25, 0.35)$, corresponding to $\delta \in (0.3, 0.5)$. Note that for the single-layer $t$-$J$ model, the pairing strength in such a heavily overdoped region is very weak [3].

The superexchange terms in Eq. (2) can be decomposed by the following intralayer and interlayer bonding and pairing order parameters:

$$\begin{aligned}
\chi^{(\alpha)}_{ij} &= \langle f^\dagger_{j\alpha\uparrow} f_{i\alpha\uparrow} + f^\dagger_{j\alpha\downarrow} f_{i\alpha\downarrow} \rangle \equiv \chi^{(\alpha)}_{j-i}, \\
\Delta^{(\alpha)}_{ij} &= \langle f_{j\alpha\downarrow} f_{i\alpha\uparrow} - f_{j\alpha\uparrow} f_{i\alpha\downarrow} \rangle \equiv \Delta^{(\alpha)}_{j-i}, \\
\chi_{i,\perp} &= \langle f^\dagger_{i2\uparrow} f_{i1\uparrow} + f^\dagger_{i2\downarrow} f_{i1\downarrow} \rangle \equiv \chi_z, \\
\Delta_{i,\perp} &= \langle f_{i2\downarrow} f_{i1\uparrow} - f_{i2\uparrow} f_{i1\downarrow} \rangle \equiv \Delta_z,
\end{aligned} \tag{3}$$

which are assumed to be site independent. The five pairing order parameters are marked in the inset of Fig. 2.

The ground-state phase diagram with respect to the filling $x$ and $J_\perp/J_\parallel$ is shown in Fig. 2(a). As $J_\perp$ should be larger than $J_\parallel$, we have set $J_\perp/J_\parallel \in (1, 2)$ in the phase diagram. Three different phases exist in Fig. 2(a). The lower right region (defined as region III) wherein the filling is relatively high and $J_\perp/J_\parallel$ is relatively small is occupied by the $d$-wave pairing. This region can be continuously connected to the low hole-doped single-layered $t$-$J$ model representing cuprates. The upper left region wherein the filling is relatively low and $J_\perp/J_\parallel$ is relatively large

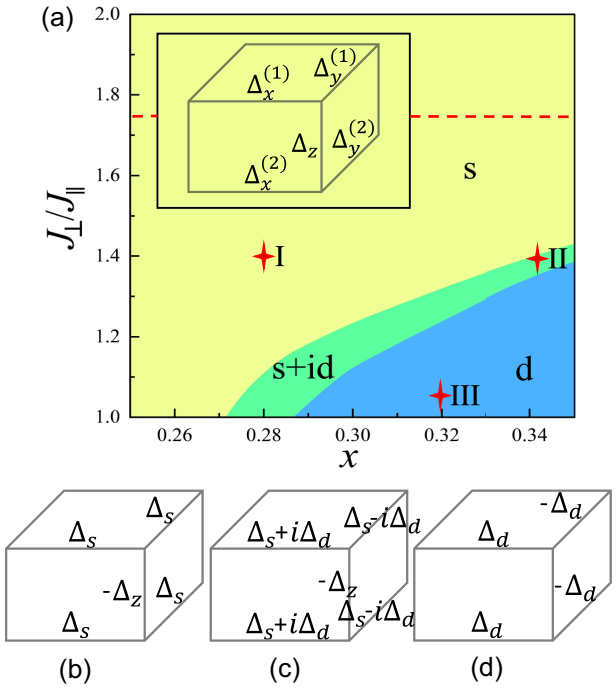


FIG. 2. (a) Ground state phase diagram with respect to the filling $x$ and $J_\perp/J_\parallel$ with $J_\parallel = 0.4t$. The inset shows the pairing order parameters. At point I (0.28,1.4): $\Delta_z = 3.5 \times 10^{-3}$, $\Delta_x^{(1,2)} = \Delta_y^{(1,2)} = -2.7 \times 10^{-5}$. At point II (0.342,1.39): $\Delta_z = 3.7 \times 10^{-2}$, $\Delta_x^{(1,2)} = \Delta_y^{(1,2)*} = (-0.36 + 4.4i) \times 10^{-3}$. At point III (0.32,1.05): $\Delta_z = 0$, $\Delta_x^{(1,2)} = -\Delta_y^{(1,2)} = 5.3 \times 10^{-3}$. The red dashed line marks the realistic $J_\perp/J_\parallel \approx 1.75$ for LNO. (b)–(d) The pairing configurations of the $s$ wave (I), $s + id$ wave (II), and $d$ wave (III), respectively.

(defined as region I) shows the $s$-wave pairing. This region is relevant to LNO, wherein $J_\perp/J_\parallel \approx 1.75$ (red dashed line); see the estimation below. Note that a variant of the bilayer Hubbard model has been simulated by the sign-free quantum Monte-Carlo approach, also showing the extended $s$-wave pairing [41]. Remarkably, a narrow region (defined as region II) sitting in between regions I and III is occupied by the $s + id$-wave pairing.

To gain more information of the pairing nature, one typical point is taken within each region in Fig. 2(a) to provide the pairing configurations. At the typical point in region I showing the $s$-wave pairing, $\Delta_z = 3.5 \times 10^{-3}$, $\Delta_x^{(1,2)} = \Delta_y^{(1,2)} = -2.7 \times 10^{-5}$, schematically shown in Fig. 2(b). Consequently, the order parameters in the two layers are in phase, and the interlayer pairing dominates the intralayer one. It is interesting to note that $\Delta_z$ and $\Delta_{x,y}^{(1,2)}$ hold different signs, which can be thought of as the residue of the $d$-wave pairing from the side view. At the typical point in region III exhibiting the $d$-wave pairing, $\Delta_z = 0$, $\Delta_x^{(1,2)} = -\Delta_y^{(1,2)} = 5.3 \times 10^{-3}$, schematically shown in Fig. 2(d). It turns out that the $d$-wave pairing order parameters on the two layers are in phase, and the interlayer pairing vanishes as it is inconsistent

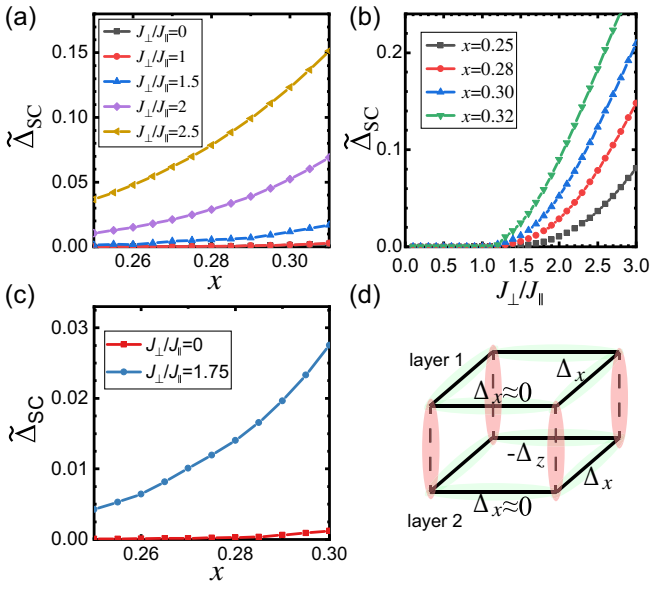


FIG. 3. (a) Ground state superconducting order parameter $\tilde{\Delta}_{SC}$ versus filling $x$ at $J_\parallel = 0.4t$ for different coupling ratios $J_\perp/J_\parallel = 0$, 1, 1.5, 2, 2.5. (b) $\tilde{\Delta}_{SC}$ versus $J_\perp/J_\parallel$ for different filling $x = 0.25$, 0.28, 0.3, 0.32. (c) Comparison of $\tilde{\Delta}_{SC}$ versus filling $x$ between $J_\perp/J_\parallel = 0$ and $J_\perp/J_\parallel = 1.75$. (d) Pairing configuration of the obtained interlayer-$s$-wave pairing for $J_\perp/J_\parallel = 1.75$.

with this symmetry. At the typical point in region II exhibiting the $s + id$-wave pairing, $\Delta_z = 3.7 \times 10^{-2}$, $\Delta_x^{(1,2)} = \Delta_y^{(1,2)*} = (-0.36 + 4.4i) \times 10^{-3}$. This pairing configuration is schematically shown in Fig. 2(c), which can be decomposed as $\Delta_s + i\Delta_d$, wherein the schematic pairing configurations for $\Delta_s$ and $\Delta_d$ are the same as Figs. 2(b) and 2(d). The $s + id$ pairing state in the intermediate regime spontaneously breaks time-reversal symmetry. A similar $s + id$ state has been suggested in the much larger filling (or much lower doping) and much smaller $J_\perp$ regime [42–44]. Such a state could induce a nontrivial supercurrent due to spatial inhomogeneity, which can be experimentally detected [45].

*Interlayer coupling driven SC.*—In the SBMF theory, the onset of SC requires the condensation of holons and the pairing of spinons. The ground state SC order parameter is denoted by $\tilde{\Delta}_{SC} = \delta\Delta_{pair}$, where $\delta$ represents the holon density and $\Delta_{pair}$ represents the spinon pairing defined in Eq. (3). We would focus on the dominant channel, either the interlayer or the intralayer one. The obtained dominant $\tilde{\Delta}_{SC}$ as a function of the filling level $x$ is plotted in Fig. 3(a) for various interlayer superexchange strengths $J_\perp/J_\parallel$ in comparison to the case of $J_\perp = 0$. Obviously, $\tilde{\Delta}_{SC}$ rises promptly with the increase of $x$ for all values of $J_\perp/J_\parallel$. This feature is similar to the case of $J_\perp = 0$ representing the single-layer $t$-$J$ model, wherein $\tilde{\Delta}_{SC}$ drops rapidly as $\delta$ approaches 0.5, or, equivalently, $x \to 0.25$. $\tilde{\Delta}_{SC}$ as a function of $J_\perp/J_\parallel$ is shown in Fig. 3(b) for specific fillings $x$. Notably, $\tilde{\Delta}_{SC}$ increases monotonically and significantly with the increase of $J_\perp/J_\parallel$ for $J_\perp > J_\parallel$ across all these experimentally relevant fillings.

The results shown in Figs. 3(a) and 3(b) are consistent with the important experimental observation in LNO [14] that the robust SC only emerges under pressure because of the following two reasons. Firstly, pressure enhances the interlayer coupling and hence $J_\perp/J_\parallel$, leading to the drastic enhancement of $\tilde{\Delta}_{SC}$ as shown in Fig. 3(b). Secondly, pressure enhances the hybridization between the $3d_{x^2-y^2}$ and the $3d_{z^2}$ orbitals [33], leading to the increasing of $x$, which also strongly enhances the $\tilde{\Delta}_{SC}$ as shown in Fig. 3(a). Furthermore, these results are also consistent with the experiment's result that the apical-oxygen vacancies suppress SC promptly [14]. In our theory, this is because vacancies break the Ni—O—Ni bonding along the $z$ axis, and hence $J_\perp$ vanishes locally, which is harmful for SC. Besides, Figs. 3(a) and 3(b) further indicate that electron doping into LNO will effectively enhance $\tilde{\Delta}_{SC}$, while hole doping will suppress $\tilde{\Delta}_{SC}$.

The value of $J_\perp/J_\parallel$ in LNO under pressure can be estimated from DFT calculations. The interlayer hopping integral of the $3d_{z^2}$ orbital is about 0.635 eV, and the intralayer NN hopping integral of the $3d_{x^2-y^2}$ is about 0.48 eV [18]. Considering the Hubbard $U$ of the two orbitals is close, we have $J_\perp/J_\parallel \approx 1.75$. Figure 3(c) shows the comparison of the filling dependence of $\tilde{\Delta}_{SC}$ between $J_\perp = 0$ and the realistic $J_\perp$, which suggests that near $x = 0.25$, the $\tilde{\Delta}_{SC}$ at $J_\perp/J_\parallel = 1.75$ is more than 1 order of magnitude higher than that at $J_\perp = 0$. The pairing symmetry for $J_\perp/J_\parallel = 1.75$ in an experimentally relevant filling regime is $s$ wave, consistent with Fig. 2(a). The corresponding pairing configuration is shown in Fig. 3(d), wherein $\Delta_x \approx 0$. Therefore, for these realistic parameters in LNO, the pairing state is the interlayer $s$-wave pairing.

Here the interlayer pairing overwhelms the intralayer one as the former suffers from less pairing frustration than the latter. For intralayer pairing, an electron has to choose one among the four surrounding NN sites to pair, which compete with one another. Instead for interlayer pairing, it can focus on the only one along the rung to pair. This not only makes $\Delta_z \gg \Delta_x$, but also greatly enhances $\Delta_z$. Therefore, the interlayer pairing mechanism leads to the robust interlayer $s$-wave pairing.

In accordance with the strong enhancement of the ground-state $\tilde{\Delta}_{SC}$ by strong $J_\perp$, the superconducting $T_c$ is also strongly enhanced proportionally within the BCS theory. In the SBMF theory, $T_c$ is given by the lower one of $T_{BEC}$ and $T_{pair}$. Here, $T_{BEC}$ represents the BEC temperature of holons, which is high due to the large doping level of the $d_{x^2-y^2}$ orbital. Conversely, $T_{pair}$, the pairing temperature of spinons, represents the physical $T_c$. $T_{pair}$ can be obtained by solving the finite-temperature MF self-consistent gap equation, which turns out to be strongly enhanced by strong $J_\perp$ (see the Supplemental Material, Sec. D [40]). Although the bilayer $t$-$J$ model studied here is a rigorous

2D system, a weak interbilayer coupling always exists in real materials, which would stabilize the long-range phase coherence [46] below a finite $T_c$ near our MF prediction.

*Discussion and conclusion.*—The role of the ligand oxygen $2p$ orbitals has been so far neglected, while previous studies proposed that based on the Ni $3d^{8+}$ configuration, i.e., one hole in each Ni $E_g$ orbital, the extra doped holes go to the ligand $2p$ orbitals [27,47,48]. Calculations show that a singly occupied $E_g$ orbital can form a Zhang-Rice singlet (ZRS) with a ligand hole [27], and then the ZRS is mapped to a "hole" similar to the case of cuprates; otherwise, it is "occupied." In this way the Ni—O system is reduced to an effective $E_g$-orbital model with occupations the same as those in Eq. (1), which justifies our starting point.

In bilayer and trilayer high $T_c$ cuprates (e.g., $YBa_2Cu_3O_{7-\delta}$ and $Bi_2Sr_2Ca_2Cu_3O_{10+\delta}$), the $d$-wave pairing takes place inside each layer. The interlayer Josephson coupling enhances SC phase coherence and increases $T_c$ by a factor of 2 or 3 [49–51]. The situation here is distinct: The strong interlayer superexchange interaction in the $3d_{x^2-y^2}$ orbital assisted by Hund's rule coupling not only renders the interlayer pairing, but also strongly enhances the pairing strength and hence the $T_c$.

*Note added.*—Note that a recent study [32] on our model, Eq. (2), adopting state-of-the-art tensor-network methods has obtained similar results as we have here.

We are grateful to Wei Li, Yi-Zhuang You, Yang Qi, Yi-Fan Jiang, and Wei-Qiang Chen for stimulating discussions. C. W. is supported by the National Natural Science Foundation of China under the Grants No. 12234016 and No. 12174317. F. Y. is supported by the National Natural Science Foundation of China under the Grant No. 12074031. C. L. is supported by the National Natural Science Foundation of China under Grant No. 12304180. This work has been supported by the New Cornerstone Science Foundation.

*These two authors contributed equally to this work.
†yangfan_blg@bit.edu.cn
‡wucongjun@westlake.edu.cn

[1] J. G. Bednorz and K. A. Müller, Z. Phys. B Condens. Matter **64**, 189 (1986).
[2] P. W. Anderson, Science **235**, 1196 (1987).
[3] G. Kotliar and J. Liu, Phys. Rev. B **38**, 5142 (1988).
[4] P. A. Lee, N. Nagaosa, and X.-G. Wen, Rev. Mod. Phys. **78**, 17 (2006).
[5] B. Keimer, S. A. Kivelson, M. R. Norman, S. Uchida, and J. Zaanen, Nature (London) **518**, 179 (2015).
[6] C. Proust and L. Taillefer, Annu. Rev. Condens. Matter Phys. **10**, 409 (2019).
[7] V. I. Anisimov, D. Bukhvalov, and T. M. Rice, Phys. Rev. B **59**, 7901 (1999).
[8] D. Li, K. Lee, B. Y. Wang, M. Osada, S. Crossley, H. R. Lee, Y. Cui, Y. Hikita, and H. Y. Hwang, Nature (London) **572**, 624 (2019).
[9] L.-H. Hu and C. Wu, Phys. Rev. Res. **1**, 032046(R) (2019).
[10] G.-M. Zhang, Y.-F. Yang, and F.-C. Zhang, Phys. Rev. B **101**, 020501(R) (2020).
[11] A. S. Botana, F. Bernardini, and A. Cano, J. Exp. Theor. Phys. **132**, 618 (2021).
[12] S. Zeng, C. Li, L. E. Chow, Y. Cao, Z. Zhang, C. S. Tang, X. Yin, Z. S. Lim, J. Hu, P. Yang, and A. Ariando, Sci. Adv. **8**, eabl9927 (2022).
[13] C. Lu, L.-H. Hu, Y. Wang, F. Yang, and C. Wu, Phys. Rev. B **105**, 054516 (2022).
[14] H. Sun, M. Huo, X. Hu, J. Li, Z. Liu, Y. Han, L. Tang, Z. Mao, P. Yang, B. Wang, J. Cheng, D.-X. Yao, G.-M. Zhang, and M. Wang, Nature (London) **621**, 493 (2023).
[15] Z. Liu, M. Huo, J. Li, Q. Li, Y. Liu, Y. Dai, X. Zhou, J. Hao, Y. Lu, M. Wang, and H.-H. Wen, arXiv:2307.02950.
[16] J. Hou, P.-T. Yang, Z.-Y. Liu, J.-Y. Li, P.-F. Shan, L. Ma, G. Wang, N.-N. Wang, H.-Z. Guo, J.-P. Sun, Y. Uwatoko, M. Wang, G.-M. Zhang, B.-S. Wang, and J.-G. Cheng, Chin. Phys. Lett. **40**, 117302 (2023).
[17] Y. Zhang, D. Su, Y. Huang, H. Sun, M. Huo, Z. Shan, K. Ye, Z. Yang, R. Li, M. Smidman, M. Wang, L. Jiao, and H. Yuan, arXiv:2307.14819.
[18] Z. Luo, X. Hu, M. Wang, W. Wú, and D.-X. Yao, Phys. Rev. Lett. **131**, 126001 (2023).
[19] Y. Zhang, L.-F. Lin, A. Moreo, and E. Dagotto, Phys. Rev. B **108**, L180510 (2023).
[20] Q.-G. Yang, D. Wang, and Q.-H. Wang, Phys. Rev. B **108**, L140505 (2023).
[21] F. Lechermann, J. Gondolf, S. Bötzel, and I. M. Eremin, Phys. Rev. B **108**, L201121 (2023).
[22] H. Sakakibara, N. Kitamine, M. Ochi, and K. Kuroki, Phys. Rev. Lett. **132**, 106002 (2024).
[23] Y. Gu, C. Le, Z. Yang, X. Wu, and J. Hu, arXiv:2306.07275.
[24] Y. Shen, M. Qin, and G.-M. Zhang, Chin. Phys. Lett. **40**, 127401 (2023).
[25] V. Christiansson, F. Petocchi, and P. Werner, Phys. Rev. Lett. **131**, 206501 (2023).
[26] D. A. Shilenko and I. V. Leonov, Phys. Rev. B **108**, 125105 (2023).
[27] W. Wú, Z. Luo, D.-X. Yao, and M. Wang, arXiv:2307.05662.
[28] Y. Cao and Y. F. Yang, Phys. Rev. B **109**, L081105 (2024).
[29] X. Chen, P. Jiang, J. Li, Z. Zhong, and Y. Lu, arXiv:2307.07154.
[30] Y.-B. Liu, J.-W. Mei, F. Ye, W.-Q. Chen, and F. Yang, Phys. Rev. Lett. **131**, 236002 (2023).
[31] H. Oh and Y.-H. Zhang, Phys. Rev. B **108**, 174511 (2023).
[32] X.-Z. Qu, D.-W. Qu, J. Chen, C. Wu, F. Yang, W. Li, and G. Su, Phys. Rev. Lett. **132**, 036502 (2024).
[33] Y. F. Yang, G. M. Zhang, and F.-C. Zhang, Phys. Rev. B **108**, L201108 (2023).
[34] V. Pardo and W. E. Pickett, Phys. Rev. B **83**, 245128 (2011).
[35] M. U. Ubbens and P. A. Lee, Phys. Rev. B **50**, 438 (1994).
[36] A. Bohrdt, L. Homeier, C. Reinmoser, E. Demler, and F. Grusdt, Ann. Phys. (Amsterdam) **435**, 168651 (2021).
[37] A. Bohrdt, L. Homeier, I. Bloch, E. Demler, and F. Grusdt, Nat. Phys. **18**, 651 (2022).

[38] S. Hirthe, T. Chalopin, D. Bourgund, P. Bojović, A. Bohrdt, E. Demler, F. Grusdt, I. Bloch, and T. A. Hilker, Nature (London) **613**, 463 (2023).
[39] A. Auerbach, *Interacting Electrons and Quantum Magnetism*, corr., 2. print ed., Graduate Texts in Contemporary Physics (Springer, New York, Berlin Heidelberg, 1998).
[40] See Supplemental Material at http://link.aps.org/supplemental/10.1103/PhysRevLett.132.146002 for additional information.
[41] T. Ma, D. Wang, and C. Wu, Phys. Rev. B **106**, 054510 (2022).
[42] Y. Suzumura, Y. Hasegawa, and H. Fukuyama, J. Phys. Soc. Jpn. **57**, 2768 (1988).
[43] K. Kuboki and P. A. Lee, J. Phys. Soc. Jpn. **64**, 3179 (1995).
[44] H. Zhao and J. R. Engelbrecht, Phys. Rev. B **71**, 054508 (2005).
[45] W.-C. Lee, S.-C. Zhang, and C. Wu, Phys. Rev. Lett. **102**, 217002 (2009).
[46] T. K. Kopeć and T. P. Polak, Phys. Rev. B **62**, 14419 (2000).
[47] T. Mizokawa, D. I. Khomskii, and G. A. Sawatzky, Phys. Rev. B **61**, 11263 (2000).
[48] V. Bisogni, S. Catalano, R. J. Green, M. Gibert, R. Scherwitzl, Y. Huang, V. N. Strocov, P. Zubko, S. Balandeh, J.-M. Triscone, G. Sawatzky, and T. Schmitt, Nat. Commun. **7**, 13017 (2016).
[49] S. Chakravarty, H.-Y. Kee, and K. Völker, Nature (London) **428**, 53 (2004).
[50] C. Chu, L. Deng, and B. Lv, Physica (Amsterdam) **514C**, 290 (2015).
[51] X. Luo *et al.*, Nat. Phys. **19**, 1841 (2023).